Jpn. J. Appl. Phys. Vol. 39 (2000) pp. 3883–3887
Part 1, No. 7A, July 2000

Heat Treatment with High-Pressure H_2O Vapor of Pulsed Laser Crystallized Silicon Films

Katsumi ASADA, Keiji SAKAMOTO, Tadashi WATANABE, Toshiyuki SAMESHIMA and Seiichiro HIGASHI[1]
Tokyo University of Agriculture and Technology, 2-24-16 Nakamachi, Koganei, Tokyo 184-8588, Japan
[1]*SEIKO EPSON Corporation, Nagano 392-8502, Japan*

(Received October 29, 1999; accepted for publication March 27, 2000)

Improvement of electrical properties for 7.4×10^{17} cm^{-3} phosphorus-doped pulsed laser crystallized silicon films of 50 nm thickness formed on quartz glass substrates was achieved by heat treatment with high-pressure H_2O vapor. The electrical conductivity was increased from 1.3×10^{-5} S/cm (as-crystallized) to 2 S/cm by annealing at 270°C for 3 h with 1.3×10^6 Pa H_2O vapor. The spin density of undoped laser crystallized silicon films was reduced from 1.6×10^{18} cm^{-3} (as-crystallized) to 1.2×10^{17} cm^{-3} by annealing at 310°C for 3 h with 1.3×10^6 Pa H_2O vapor. Theoretical analysis revealed that the potential barrier height at grain boundaries decreased from 0.3 eV (as-crystallized) to 0.002 eV. High-pressure H_2O vapor annealing offer the possibility of reducing the density of defects states through oxidation of the defects at low temperature.

KEYWORDS: laser crystallization, activation energy, defect density, carrier density, potential barrier height

1. Introduction

Redction of defects in silicon films at low temperatures is very important for fabrication of electronic devices, such as, thin film transistors (TFTs) and solar cells.[1–3] We have proposed a simple heat treatment with high-pressure H_2O vapor for this purpose.[4] Reduction of the threshold voltage and increase of the effective mobility of polycrystalline silicon thin film transistors (poly-Si TFTs) have been observed by heat treatment with high-pressure H_2O vapor.[5] We have also demonstrated the improvement of electrical properties of SiO_2 films, SiO_2/Si interfaces and poly-Si films by the reduction of the density of trapped states and fixed oxide charges.[6–8]

In this paper, we discuss the carrier generation and reduction of defects for lightly phosphorus-doped pulsed laser crystallized silicon films by heat treatment with high-pressure H_2O vapor. Change in the electrical conductivity caused by reduction of the density of localized defect states is presented. Reduction of the spin density is also reported for undoped films. We also discuss the electrical conductivity of the polycrystalline films using a statistical thermodynamical calculation program.

2. Experimental

Undoped and phosphorus-doped 50-nm-thick amorphous silicon films with a density of 7.4×10^{17} cm^{-3} were formed on glass substrates using low-pressure chemical vapor deposition (LPCVD) and ion implantation methods. The samples were placed in a vacuum chamber, which was evacuated by a turbomolecular pump to a level of 1×10^{-4} Pa for laser irradiation. Polycrystalline silicon films were fabricated through rapid melt-regrowth induced by 28 ns pulsed XeCl excimer laser heating. Multiple-step-laser energy irradiation was carried out. Laser energy density was increased from 160 mJ/cm^2 (crystallization threshold) to 400 mJ/cm^2 in 20 mJ/cm^2 steps. Five pulses were irradiated at each laser energy density step. Samples were then placed in a pressure-proof stainless-steel chamber with a metal seal. Purified water was also put into the chamber before sealing. The chamber was then placed on a hot plate to heat the samples at 190–310°C. The water evaporated during heating and the gas pressure increased. After heat treatment, Al electrodes were formed on phosphorus-doped polycrystalline films to measure the change in the electrical conductivity under heat treatment conditions in the presence of H_2O vapor. The spin density was also measured by the electron spin resonance (ESR) microwave absorption method for undoped polycrystalline films formed by laser irradiation before and after heat treatment.

3. Results and Discussion

Figure 1 shows the electrical conductivity as a function of the heating temperature with 1.3×10^6 Pa H_2O vapor for 1 h and 3 h for samples crystallized at a laser energy density of 400 mJ/cm^2, in vacuum at room temperature. Although in general most of the phosphorus atoms are incorporated in crystalline silicon lattice sites by pulsed laser induced melting followed by solidification, the samples just after crystallization had a low electrical conductivity of 1.3×10^{-5} S/cm. This indicates that the pulsed laser crystallized silicon films had a high density of defect states at deep energy levels near the mid gap region. The defect states localized at grain boundaries and they trapped most of the electrons generated from ionized phosphorus atoms in crystalline grains.[9–12] The electrical conductivity was markedly increased by heat treatment with high-pressure H_2O vapor from 190 to 310°C, as shown in Fig. 1. The electrical conductivity reached a max-

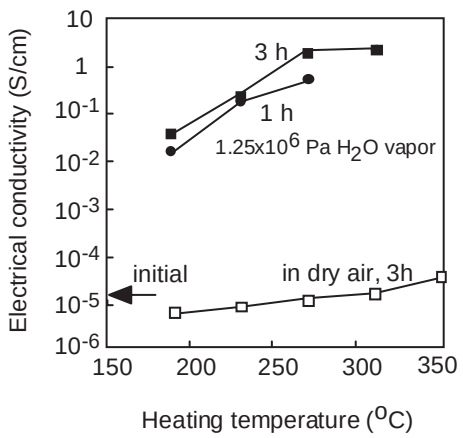

Fig. 1. Electrical conductivity as a function of temperature of heat treatment with 1.3×10^6 Pa H_2O vapor for 1 h and 3 h for 7.4×10^{17} cm^{-3} phosphorus-doped silicon films of 50 nm thickness crystallized at laser energy densities of 400 mJ/cm^2 (solid marks) and as a function of temperature of heat treatment in dry air (open marks). Electrical conductivity for as-crystallized films is also shown.

imum of 2 S/cm for heat treatment at 270°C for 3 h. Figure 1 also shows the change in electrical conductivity as a function of heating temperature for 3 h in dry air (humidity 20%). No marked increase in the electrical conductivity was observed under these conditions for the entire heating temperature range. These results clearly show that the electrical properties of the laser crystallized silicon films were markedly changed by heat treatment with high-pressure H_2O vapor in the temperature range from 190 to 310°C, although the simple heating in dry atmosphere yielded no appreciable change for the entire temperature range considered. Figure 2 shows changes in the electrical conductivity as a reciprocal function of temperature for initial laser crystallized silicon films and films annealed with H_2O vapor at 190 and 270°C for 1 h and 3 h, respectively. The low electrical conductivity of the initial crystallized films increased with an activation energy of 0.55 eV as the temperature increased. On the other hand, the electrical conductivity increased and the activation energy decreased after heat treatment with high-pressure H_2O vapor. This result indicates that the free carrier density increased after heat treatment. ESR measurements were conducted to measure the spin density for undoped silicon films laser crystallized at 400 mJ/cm^2 before and after heat treatment with high-pressure H_2O vapor. Figure 3 shows the spin density as a function of heating temperature for heat treatment at 1.3×10^6 Pa for 3 h. The initial films crystallized at 400 mJ/cm^2 and had a high spin density of 1.6×10^{18} cm^{-3} caused by dangling bonds localized at grain boundaries.[13,14] The spin density was reduced to 1.2×10^{17} cm^{-3} by heat treatment as the heating temperature was increased to 310°C. The dangling bond was effectively passivated by heat treatment with high-pressure H_2O vapor.

Figures 1–3 reveal that the heat treatment with H_2O vapor caused the defects to be electrically inactive and changed localized electron states to extended states. Defect states localized at grain boundaries for laser crystallized silicon films reacted with H_2O molecules incorporated into silicon films. H_2O molecules at defect sites would be chemically dissociated with the help of heating energy. The dangling bonds of silicon atoms were probably eliminated through the formation of Si–O, Si–OH or Si–H bonds.

In order to understand the change in the electrical properties, we developed a statistical thermodynamical program for analysis of the electrical conductivity of polycrystalline films.[15–17] We introduced a Gaussian-type energy distribution of the density of defect states in the band gap, whose energy level at the maximum density and the width can be changed. We hypothesized that defect states localized at grain boundaries and grain boundary planes had a certain defect density per unit area. We also used the average volume density of the defect states in crystalline grains in order to compare the dopant ion and free electron carrier volume densities. The average volume density of the defect states was calculated from the defect density per unit area divided by the average grain size. Phosphorus dopant atoms were assumed to be distributed uniformly in silicon films. Electron carriers are generated from the phosphorus dopant atoms via their ionization The electron generation probability is determined with the Fermi-Dirac statistical distribution function. Free carriers are trapped by the localized defect states and the defects are negatively charged. The Fermi energy level and the free carrier density at the center point of crystalline grains are determined by the statistical thermodynamical conditions which maintain the charge neutrality among the densities of ionized dopant atoms (N_d), negatively charged defect states with electron carriers (X_d) and free carriers (n) ($N_d = n + X_d$) in the entire region including crystalline grains and grain boundaries. However, the density of ionized donors is larger that that of free electrons in crystalline grains because some electrons produced from doped phosphorus atoms are trapped at grain boundaries, although charge neutrality is always maintained in the entire semiconductor region. This space charge effect in crystalline grains causes band bending and results in the potential barrier at grain boundaries, which is determined by the difference in potential at the conduction band edge between the center point of the crystalline grains and their boundaries. The potential energy, $\phi(x)$, at x, which is the distance from the center point of the crystalline grain, is calculated using the Poisson equation with the density of space charges ($N_d - n$) as

$$\frac{\partial^2 \phi(x)}{\partial x^2} = \frac{e(N_d - n)}{\epsilon_s \epsilon_o}, \tag{1}$$

where e is the elemental charge, ϵ_o is the vacuum dielectric constant and ϵ_s is the dielectric permittivity of silicon. The carrier density $n(x)$ of the crystalline grain is given as

$$n(x) = N_c \exp\left(\frac{-e(E_g - E_f + \phi(x))}{kT}\right), \tag{2}$$

where N_c is the effective density of states at the conduction band, E_g is the energy band gap, E_f is the height of the Fermi level from the valence band edge to the center point of the crystalline grains, k is the Boltzmann constant and T is the absolute temperature. The effective carrier density in the lateral direction was calculated because the band bending causes a distribution of the free carrier density in the lateral direction. The effective carrier density in the lateral direction, $n_{lateral}$, is obtained from integration of the reciprocal number of carrier density from the center point to the grain boundary as,

$$n_{lateral} = \left(\frac{2}{L}\int_0^{\frac{L}{2}} \frac{1}{n(x)} dx\right)^{-1}, \tag{3}$$

where L is the average crystalline grain size. If there is a high potential barrier at grain boundaries, the carrier density is very low at the boundaries, so that the effective carrier density in the lateral direction becomes much lower than the average free carrier density in crystalline grains.

Heat treatment with high-pressure H_2O vapor was introduced in the calculation program. The density of H_2O molecules is assumed to distribute as the complementary error function in the depth direction. The density of the defect states is assumed to be reduced in proportion to the reaction probability and the density of H_2O molecules incorporated in the films as shown by the following equation.

$$\frac{dn_d}{dt} = -pF, \tag{4}$$

$$F = F_0 \,\mathrm{erft}\frac{x}{2\sqrt{Dt}}, \tag{5}$$

where n_d is the density of defect states, p is the reaction probability, F_0 is the H_2O flux entiring into silicon films and D is the diffusion coefficient of H_2O molecules into silicon films.

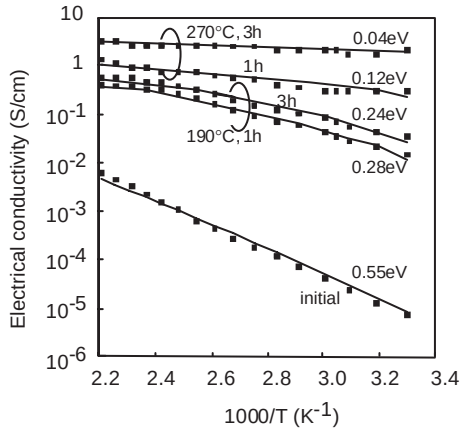

Fig. 2. Temperature dependence of the electrical conductivity of 7.4×10^{17} cm^{-3} phosphorus-doped 50-nm-thick silicon films laser crystallized at 400 mJ/cm^2 as a reciprocal function of temperature. Heat treatments were carried out with 1.3×10^6 Pa H_2O vapor. Solid curves show the temperature dependence of the electrical conductivity calculated using our program including the space charge effect caused by defect states trapping electrons at grain boundaries. Defect states with an energy level of 0.2 eV above the mid gap region and a width of 0.4 eV, an average grain size of 45 nm and an H_2O diffusion coefficient of 3×10^{-15} cm^2/s were used. Activation energy is presented for each fabrication condition.

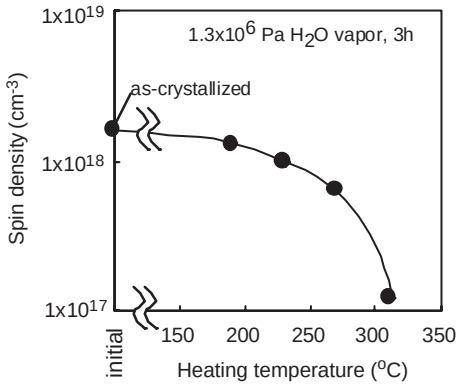

Fig. 3. The spin density of undoped 50-nm-thick silicon films laser crystallized at 400 mJ/cm^2 as a function of heating temperature. Heat treatment was carried out with 1.3×10^6 Pa H_2O vapor for 3 h.

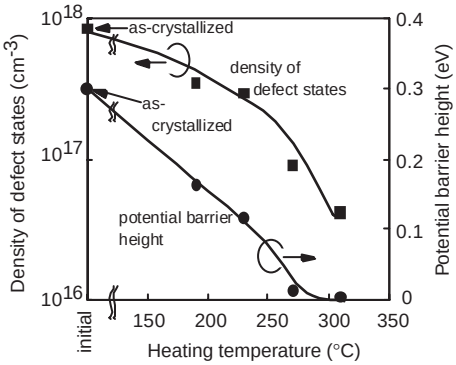

Fig. 4. Density of defect states and potential barrier height at grain boundaries and calculated with conditions of 7.4×10^{17} cm^{-3} phosphorus doping, defect states with an energy level of 0.2 eV above the mid gap region and a width of 0.4 eV, an average grain size of 45 nm and an H_2O diffusion coefficient of 3×10^{-15} cm^2/s as functions of heating temperature for heat treatment with 1.3×10^6 Pa H_2O vapor for 3 h.

We also introduce scattering effects due to dopant ions, lattice vibration and disordered states at grain boundaries, which reduce the carrier mobility. We used the carrier scattering effect of dopant ions and lattice vibration, reported by Irvin and Prince,[18,19] while the mobility reduction rate due to lattice disordered states was determined by the fitting between experimental and calculated conductivity. Through the fitting between temperature dependences of calculated and experimental conductivities for the initial as-crystallized case shown in Fig. 2, the energy level and width of defect states were determined as 0.2 eV above the mid gap and 0.4 eV, respectively. Then the H_2O flux, the reaction probability and the H_2O diffusion coefficient were obtained by fitting activation energies of change in the calculated electrical conductivity to experimental ones for every temperature. The value of H_2O flux x reaction probability [pF_0 in eqs. (4) and (5)] increased from 5.3×10^{13} to 8.3×10^{13} cm^{-3}/s as the heating temperature increased from 190 to 310°C. The H_2O diffusion coefficient also increased from 3×10^{-15} to 6×10^{-15} cm^2/s, as the heating temperature increased from 190 to 310°C. Finally the mobility reduction rate due to scattering at grain boundaries (0–1) was determined by agreement between experimental and calculated conductivities for every temperature and every duration of heat treatment with high-pressure H_2O vapor to give the carrier mobility of the poly-Si films shown in Fig. 2.

Our analysis gave an initial density of defect states of 8.4×10^{17} cm^{-3} for as-crystallized films. The density of defect states decreased to 4×10^{16} cm^{-3} as the heating temperature increased to 310°C for 1.3×10^6 Pa high-pressure H_2O vapor annealing for 3 h, as shown in Fig. 4. Although the density of defect states given by our analysis before and after heat treatment was of the same order of magnitude as the spin densities obtained by ESR measurements as shown Figs. 3 and 4, the calculated defect density was one half or one third of the experimental spin density. Experimental accuracy and simple assumptions for calculation probably resulted in a part of the difference. Moreover, we guess the defect density obtained by analysis of the electrical conductivity may be lower than the spin density because the electrical current flows along the most conductive path. A high density of defects trap free electrons and cause the band bending resulting in the potential barrier height at grain boundaries, which blocks the electrical current. For the as-crystallized case, the potential barrier height was estimated as 0.3 eV because of the high density of defects, which trapped a number of free electrons. The potential barrier height decreased to 0.002 eV according to the reduction of the density of defect states as the heating temperature increased to 310°C, as shown in Fig. 4. The potential barrier height, 0.002 eV, was low enough for most of the electrons to travel across the barrier at room temperatures. Therefore the effective free carrier density increased. Figure 5 shows the average density of free carriers existing in crystalline grains and the effective carrier density in the lateral direction, n_{lateral}. Although the average carrier density in crystalline grains was 7×10^{15} cm^{-3} for as-crystallized films, the effective carrier density in the lateral direction was only 2×10^{12} cm^{-3}. The low n_{lateral} resulted from a high potential barrier height of 0.3 eV at grain boundaries caused by the space charge effect in electron depletion regions. The Fermi level gives the free carrier density at the center point of crystalline grains, which is close to the average carrier desnity. On the other hand, n_{lateral} suffers from the potential barrier

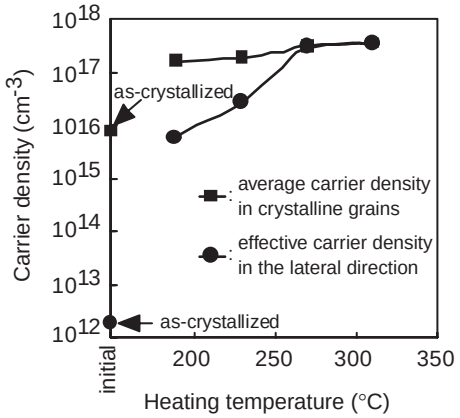

Fig. 5. Average carrier density in crystalline grains and effective carrier density in the lateral direction as functions of temperature of heat treatment with 1.3×10^6 Pa H_2O vapor for 3 h for the 400 mJ/cm^2 crystallization case. The carrier densities were obtained through a fitting between experimental and calculated electrical conductivities under the same conditions given in Fig. 4.

height. When the potential barrier height is high and the electron depletion region is thick, n_{lateral} is very low, as shown in eqs. (2) and (3). The electrical conductivity obtained by the electrical current measurements is governed by $en_{\text{lateral}}\mu$. Its activation energy was high at 0.55 eV for as crystallized films, as shown in Fig. 2. The Fermi level is positioned at 0.15 eV below the conduction band edge at the middle point of crystalline grains. On the other hand, the conduction band edge was 0.45 eV above the Fermi level at grain boundaries because of the existence of there was a potential barrier height of 0.3 eV. The activation energy, 0.55 eV, was higher than the Fermi level at grain boundaries, 0.45 eV. The high activation energy resulted from the fact that the thickness of the depletion regions formed around grain boundaries decreased as the temperature increased. Because the ionization probability of dopant atoms increased as the temperature increased, the density of electrons generated from dopant atoms increased so that the thickness of the electron depletion region decreased. The reduction of the depletion region thickness made n_{lateral} increase with the activation energy of 0.55 eV, which is higher than the energy gap between the Fermi level and the conduction band at grain boundaries. The activation energy of the electrical conductivity for doped polycrystalline silicon depends on various electrical properties, the Fermi level, the potential barrier height and the dopant ionization probability.

When the density of defect states was reduced by the heat treatment with high-pressure H_2O vapor, the number of electrons trapped at defect states also was reduced thus that the space charge effect decreased. This resulted in an increase of the average carrier density in crystalline grains. The Fermi level at the center point of the crystalline grains rose to 0.06 eV below the conduction band edge for annealing at 190°C for 3 h and to 0.05 eV for annealing at 270°C 3 h. Reduction of the density of defect states also reduced the potential barrier height at grain boundaries. Therefore, the effective carrier density in the lateral direction markedly increased and closely approached to that of the average free carrier density in crystalline grains, as shown by the cases of heat treatment with high-pressure H_2O vapor in Fig. 5. The potential barrier height was essential for carrier transportation. The carrier conductivity therefore increased and its activation energy reduced after H_2O vapor annealing as shown in Figs. 1 and 2. According to our previous study on the density of Si–H bonding, the increment of the Si-H density was less than -0.4 at.% (-2×10^{20} cm^{-3}) after heat treatment with high-pressure H_2O vapor.[13] We however believe that the present heat treatment supplies a sufficient amount of hydrogen as well as oxygen to terminate -10^{18} cm^{-3} silicon dangling bonds. The carrier mobility was estimated as 40 cm^2/Vs after heat treatment with high-pressure H_2O vapor by considering the scattering effect at grain boundaries for 7.4×10^{17} cm^{-3} phosphorus-doped silicon films.

4. Summary

High-pressure H_2O vapor annealing was used for reduction of the density of defect states of 50-nm-thick pulsed laser crystallized silicon films. The electrical conductivity of 7.4×10^{17} cm^{-3} phosphorus-doped silicon films crystallized by XeCl excimer laser irradiation at 400 mJ/cm^2 was increased from 1.3×10^{-5} (as-crystallized) to 2 S/cm by heat treatment with 1.3×10^6 Pa H_2O vapor for 3 h at 270°C. The activation energy of the temperature dependence of electrical conductivity was reduced from 0.55 eV (as-crystallized) to 0.04 eV. The spin density of undoped laser crystallized silicon films was reduced from 1.6×10^{18} cm^{-3} (as-crystallized) to 1.2×10^{17} cm^{-3} when H_2O vapor annealing was carried out at 310°C with 1.3×10^{15} Pa H_2O vapor for 3 h. A statistical thermodynamical analysis of electrical properties was conducted using experimental results. The high density of defect states resulted in localization of free electrons generated from phosphorus atoms at grain boundaries and caused a high potential barrier height of 0.3 eV for as-crystallized films. This resulted in a low effective carrier density in the lateral direction and low electrical conductivity. Heat treatment with high-pressure H_2O vapor yielded defect states electrically inactive so that most of the electrons became conductive and the potential barrier heights at grain boundaries decreased to 0.002 eV. The electrical conductivity consequently markedly increased to 2 S/cm through the heat treatment. The present results show that heat treatment with high-pressure H_2O vapor effectively reduces the density of defect states at grain boundaries of laser-crystallized silicon films.

Acknowledgements

We thank Dr. M. Kondo, Dr. A. Matsuda, Dr. T. Mohri and Professor T. Saitoh for their support.

1) N. Sano, M. Sekiya, M. Hara, A. Kohno and T. Sameshima: IEEE Electron Device Lett. **16** (1995) 157.
2) U. Mitra, B. Rossi and B. Khan: J. Electrochem. Soc. **138** (1991) 3420.
3) K. Baert, H. Murai, K. Kobayashi, H. Namizaki and M. Nunoshima: Jpn. J. Appl. Phys. **32** (1993) 2601.
4) T. Sameshima and M. Satoh: Jpn. J. Appl. Phys. **36** (1997) L687.
5) T. Sameshima, M. Satoh, K. Sakamoto, K. Ozaki and K. Saitoh: Jpn. J. Appl. Phys. **37** (1998) L1030.
6) T. Sameshima, M. Satoh, K. Sakamoto, K. Ozaki and K. Saitoh: Jpn. J. Appl. Phys. **37** (1998) 4254.
7) T. Sameshima, K. Sakamoto, Y. Tsunoda and T. Saitoh: Jpn. J. Appl. Phys. **37** (1998) L1452.
8) T. Sameshima, M. Satoh and K. Sakamoto: Thin Solid Films **335** (1998) 138.
9) D. Jousse, S. L. Delage and S. S. Iyer: Philos. Mag. B **63** (1991) 443.
10) T. Sameshima, M. Sekiya, M. Hara, N. Sano and A. Kono: J. Appl. Phys. **76** (1994) 7377.

11) S. Higashi, K. Ozaki, K. Sakamoto, Y. Kano and T. Sameshima: Jpn. J. Appl. Phys. **38** (1999) 857.
12) I. Yamamoto, H. Kuwano and Y. Saito: J. Appl. Phys. **71** (1992) 3350.
13) T. Sameshima, M. Satoh, K. Sakamoto, K. Ozaki and K. Saitoh: Jpn. J. Appl. Phys. **37** (1998) 4254.
14) W. B. Jackson, N. M. Johnson and D. K. Biegelsen: Appl. Phys. Lett. **43** (1983) 195.
15) J. Y. Seto: J. Appl. Phys. **46** (1975) 5247.
16) G. Baccarani, B. Ricco and G. Spadini: J. Appl. Phys. **49** (1978) 5565.
17) K. Sakamoto, T. Sameshima, Y. Tsunoda and S. Higashi: Proc.Workshop on Active Matrix Liquid Crystal Displays, Tokyo, Japan, 1999, p. 131.
18) J. C. Irvin: Bell Syst. Tech. J. **41** (1962) 387.
19) M. B. Prince: Phys. Rev. **94** (1954) 42.